2004

Methyl Bromide In Preindustrial Air: Measurements From an Antarctic Ice Core

Eric S. Saltzman
University of California - Irvine

Murat Aydin
University of California - Irvine

Warren J. De Bruyn
Chapman University, debruyn@chapman.edu

Daniel B. King
Drexel University

Shari A. Yvon-Lewis
NOAA

Recommended Citation

Saltzman, E. S., M. Aydin, W. J. De Bruyn, D. B. King, and S. A. Yvon-Lewis (2004), Methyl bromide in preindustrial air: Measurements from an Antarctic ice core, *J. Geophys. Res.*, 109, D05301, doi:10.1029/2003JD004157.

Methyl Bromide In Preindustrial Air: Measurements From an Antarctic Ice Core

Methyl bromide in preindustrial air: Measurements from an Antarctic ice core

Eric S. Saltzman,[1] Murat Aydin,[1] Warren J. De Bruyn,[2]
Daniel B. King,[3] and Shari A. Yvon-Lewis[4]

Received 17 September 2003; revised 2 December 2003; accepted 14 January 2004; published 2 March 2004.

[1] This paper presents the first ice core measurements of methyl bromide (CH_3Br). Samples from a shallow Antarctic ice core (Siple Dome, West Antarctica), ranging in mean gas dates from 1671 to 1942, had a mean CH_3Br mixing ratio of 5.8 ppt. These results extend the existing historical record derived from air and Antarctic firn air to about 350 years before present. Model simulations illustrate that the ice core results are consistent with estimates of the impact of anthropogenic activity (fumigation, combustion, and biomass burning) on the atmospheric CH_3Br burden, given the large current uncertainties in the modern atmospheric CH_3Br budget. A preindustrial scenario assuming no fumigation, no combustion, and a 75% reduction in biomass-burning sources yields a Southern Hemisphere mean mixing ratio of 5.8 ppt, in good agreement with the ice core results. There is a significant imbalance between the known CH_3Br sources and sinks in the modern atmospheric CH_3Br budget. The ice core data do not sufficiently constrain the model to determine how much of the "unknown source" was present in the preindustrial budget. The results do indicate that most of the southern hemispheric component of this "unknown source" is not anthropogenic. *INDEX TERMS:* 0322 Atmospheric Composition and Structure: Constituent sources and sinks; 0365 Atmospheric Composition and Structure: Troposphere—composition and chemistry; 1610 Global Change: Atmosphere (0315, 0325); 1615 Global Change: Biogeochemical processes (4805); *KEYWORDS:* methyl bromide, methyl halide, halocarbons

Citation: Saltzman, E. S., M. Aydin, W. J. De Bruyn, D. B. King, and S. A. Yvon-Lewis (2004), Methyl bromide in preindustrial air: Measurements from an Antarctic ice core, *J. Geophys. Res.*, *109*, D05301, doi:10.1029/2003JD004157.

1. Introduction

[2] Methyl bromide (CH_3Br) is a significant contributor to the stratospheric halogen burden and to stratospheric ozone depletion. As a result, industrial production of this compound has been phased out under the Amendments to the Montreal Protocol. CH_3Br is markedly different from many other regulated halogen compounds, such as CFC's, in that it has a complex biogeochemical cycle, with natural sources and sinks in both terrestrial and oceanic environments. Our understanding of the biogeochemical cycle of CH_3Br has improved in recent years, as a result of numerous field, laboratory, and modeling studies. However, the sources and sinks are still not well characterized, and there remain significant uncertainties associated with the major terms in the global atmospheric budget [*Montzka et al.*, 2003b]. These uncertainties limit our ability to predict the atmospheric impact of declining industrial production. For example, *Yokouchi et al.* [2002] and *Montzka et al.* [2003a] recently noted that the atmospheric CH_3Br decrease since 1998 is about two-fold larger than anticipated.

[3] Instrumental records of atmospheric CH_3Br extend only as far back as the late 1970s [*Khalil et al.*, 1993; *Miller*, 1998; *Montzka et al.*, 2003a]. Firn air measurements at four locations in Antarctica extend the record to the mid-1900s, and a few samples from the basal firn air at South Pole extend the record further to about 1900 [*Butler et al.*, 1999; *Sturges et al.*, 2001]. The data suggest a 1 ppt (pmol mol^{-1}) increase in Southern Hemisphere CH_3Br over the first half of the twentieth century, followed by a 2 ppt increase during the latter half of the century. While Antarctic firn air appears to contain a paleoatmospheric archive, this is not the case in Greenland. Greenland firn air exhibits evidence of in situ production, with elevated CH_3Br levels near the base of the firn [*Butler et al.*, 1999; *Sturges et al.*, 2001], and evidence of photochemical production of CH_3Br in near-surface snow [*Swanson et al.*, 2002]. The precursors and mechanisms of in situ production are not yet known.

[4] In this paper, we present the first measurements of CH_3Br in preindustrial air extracted from an Antarctic ice core. The study of polar ice cores can potentially provide a strong constraint on preindustrial atmospheric levels, and, therefore, on the atmospheric impact of anthropogenic emissions. Ice core records can also provide longer-term

[1]Earth System Science, University of California, Irvine, California, USA.
[2]Department of Physical Sciences, Chapman University, Orange, California, USA.
[3]Department of Chemistry, Drexel University, Philadelphia, Pennsylvania, USA.
[4]Atlantic Oceanographic and Meteorological Laboratory, National Oceanographic and Atmospheric Administration, Miami, Florida, USA.

0148-0227/04/2003JD004157

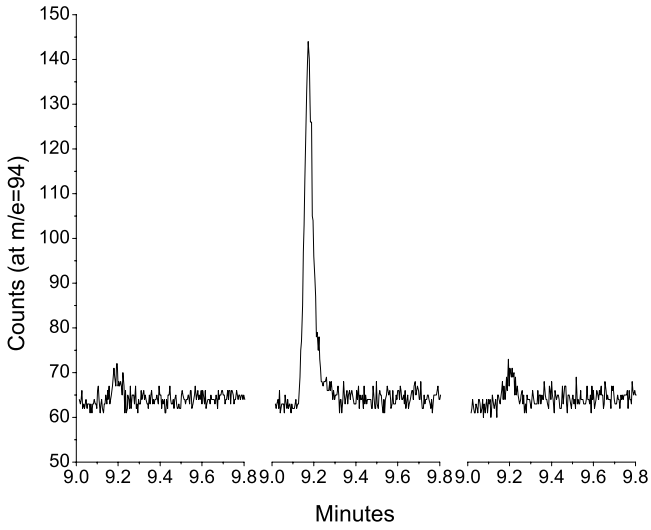

Figure 1. Selected ion-monitoring signal from GC/MS analysis of CH_3Br (m/e = 94) in a Siple Dome ice core sample (64.5 m; 750 g). (left) N_2 extraction chamber blank prior to sample extraction; (middle) 70 ml STP air extracted from the ice core sample; (right) N_2 extraction blank after extraction.

records of natural variability and insight into the sensitivity of the CH_3Br cycle to climate change.

2. Ice Core Analysis of CH_3Br

2.1. Ice Core Characteristics and Dating

[5] This study utilized samples from the Siple Dome C core drilled December 1995 at Siple Dome, West Antarctica, as part of the West Antarctic Ice Sheet program (WAISCORES). This ice core is 10 cm in diameter and was dry-drilled using an electromechanical drill to a depth of 92 meters. The core was drilled at 81.65°S, 148.81°W at 620 m above sea level, near the edge of the Ross Ice Shelf. The mean annual temperature is −25.4°C. The pore close-off depth at Siple Dome is approximately 56 m.

[6] The age of air in Siple Dome firn was determined using a 1-dimensional firn air diffusion model [*Schwander et al.*, 1988; *Schwander*, 1989; *Trudinger et al.*, 1997]. The mean age of CH_3Br in individual ice core samples was estimated by applying the ice age/gas age difference to the ice age as determined from annual layer counting (R. B. Alley, personal communication, 2003). In the firn air model, the variation of diffusivity with depth was empirically "tuned" to obtain agreement between Siple Dome firn air CO_2 profiles [*Aydin et al.*, 2004] and the atmospheric history of CO_2 [*Etheridge et al.*, 1996; *Tans et al.*, 2001]. The resultant diffusivity profile also achieved close agreement between measured firn air profiles of CFC-12 [*Butler et al.*, 1999] and the reconstructed atmospheric history of *Walker et al.* [2000]. The model was run using a mean annual snow accumulation rate of 100 kg m^{-2} yr^{-1} and a CH_3Br diffusivity in air of 9.7×10^{-6} m^2 s^{-1} [*Wilke and Lee*, 1955]. For CH_3Br, the mean ice age/gas age difference at Siple Dome is approximately 316 years, the mean gas age of firn at close-off is approximately 58 years, and the full width of the gas age distribution is about 25 years at half height.

2.2. Ice Core Gas Extraction and Analysis

[7] The air contained in 300–750 g ice core samples was extracted by mechanically shredding the ice in a stainless-steel chamber under vacuum at −48°C. The air evolved during this process (30–60 cc STP per sample) was cryogenically focused in a stainless-steel tube immersed in liquid He and analyzed using capillary gas chromatography with quadrupole mass spectrometry. CH_3Br was detected using electron impact ionization with selected ion monitoring of the parent ion (CH_3Br^+; m/e = 94). Details of the extraction, analysis, and standardization procedures are given by *Aydin et al.* [2002].

[8] The analysis of each ice core sample consisted of three steps. Prior to shredding, 50 cc STP N_2 was added to the evacuated extraction chamber containing the solid ice core sample. After 25–30 minutes, the N_2 was cryogenically removed from the chamber and analyzed, as a "pre-shredding blank." Next, the chamber was re-evacuated, the ice core sample was shredded, and the evolved air was collected and analyzed. Finally, the chamber containing the shredded ice core sample was re-evacuated, another 50 cc STP N_2 was added, and a "post-shredding blank" was obtained over the shredded ice (Figure 1). It is assumed that the ice core sample contains a blank similar to the N_2 blanks, so for each sample the mean of the two blanks was subtracted from the ice core sample signal. The uncertainties that resulted from this blank correction were mostly ±5% or lower. However, a few samples run early in the study had high blank levels and high variability between the "pre-" and "post-shredding" blanks, resulting in higher uncertainties of ±10–40%.

[9] Standardization was based on high-pressure aluminum cylinders containing 10–20 nmol mol^{-1} CH_3Br in N_2, prepared in our laboratory. These standards were diluted barometrically to 10–20 ppt with N_2 in humidified stainless-steel flasks and analyzed in the same manner as ice core samples. An informal intercalibration of our standards with NOAA/CMDL standards yielded agreement within ±3%.

2.3. Ice Core Results and Discussion

[10] Twenty-three Siple Dome ice core samples ranging in depth from 55 to 85 m were analyzed for this study. The samples had CH_3Br mixing ratios ranging from 3.2 to 9.0 ppt, with a mean and standard error of 5.8 ± 0.3 ppt (Figure 2). Three samples at 73, 74, and 83 m depth had low CH_3Br mixing ratios in the 3 to 4 ppt range. These samples also had higher analytical uncertainty than most, resulting from large blank corrections. These samples were run early in the study when the pre- and post-shredding blanks were large. More thorough baking of the extraction chamber was carried out for later samples, resulting in lower blanks. One sample at about 65 m had a CH_3Br mixing ratio of nearly 8 ppt, considerably higher than the surrounding data points. This elevated sample is not supported by the adjacent samples, as might be expected for a real atmospheric excursion. The mixing of air in the firn causes significant overlap between the age ranges of adjacent samples. Single point excursions should be viewed with caution until confirmed by additional analyses. Two data points at 79

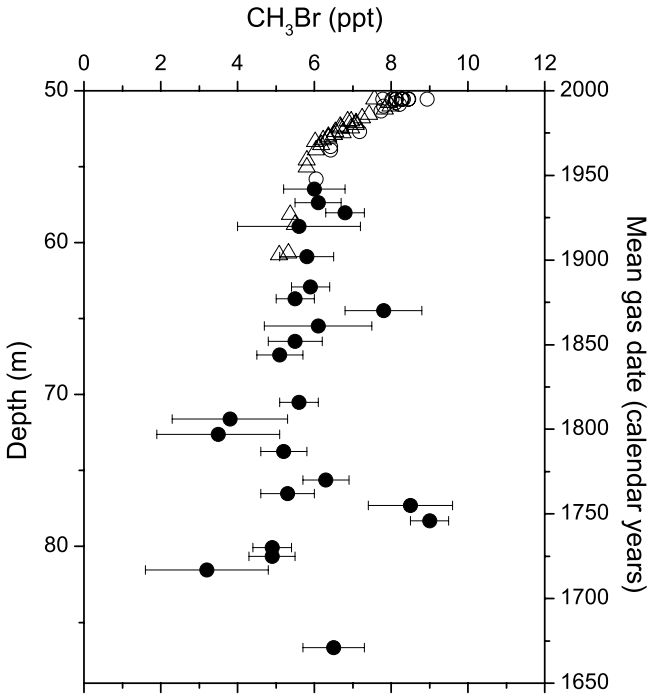

Figure 2. CH_3Br in Siple Dome ice core samples (solid circles) from this study and Siple Dome firn air (open circles) and South Pole firn air (open triangles) results from *Butler et al.* [1999] plotted against mean gas date. The depth scale applies only to the ice core data.

and 80 m had mixing ratios around 9 ppt. Although these two points are in apparent agreement with each other, diffusion modeling suggests that they are unlikely to represent a real spike in atmospheric mixing ratios. A spike in atmospheric levels large enough to cause this excursion should cause adjacent samples above and below to be elevated as well. The elevated data points may result from contamination, either during storage or during extraction and analysis in the laboratory, but there is no independent evidence for contamination of these samples.

[11] An error-weighted linear regression of all the CH_3Br data against time yields a slope of $3 \times 10^{-5} \pm 0.003$ ppt yr^{-1}, indistinguishable from zero. We recalculated the linear regression omitting the 6 outliers identified above, and the deepest point, which is more than 50 years away from the neighboring data. An error-weighted linear regression of the remaining 16 points yields a statistically significant increasing trend of 0.005 ± 0.001 ppt yr^{-1} for samples with mean CH_3Br dates ranging from 1717 to 1942 (Figure 3).

[12] Antarctic firn air CH_3Br measurements from Siple Dome and South Pole are also shown in Figure 2. The deepest sample from the Siple Dome firn has a CO_2 date of 1948, based on a comparison of the measured CO_2 mixing ratio with the atmospheric history from the well-dated Law Dome ice core [*Etheridge et al.*, 1996]. This sample has a CH_3Br mixing ratio of 6 ppt [*Butler et al.*, 1999]. Similar results were obtained by *Sturges et al.* [2001] from firn air samples of similar age collected at Dome Concordia and Dronning Maud Land, Antarctica. In agreement with the firn data, the two shallowest ice core samples from this study have 6 ppt CH_3Br with mean CH_3Br dates corresponding to 1934 and 1942. The mixing ratio of CH_3Br is slightly lower at 5.1–5.3 ppt at the bottom of the South Pole firn where the CO_2 date is just over 1900 [*Butler et al.*, 1999]. The firn data of *Butler et al.* [1999] and the trend we observed in the ice core data suggest that CH_3Br levels in the atmosphere may have been increasing slowly for about 200 years before the onset of rapid increase during the second half of the twentieth century. The average rate of increase in the ice core data is less than half of that reported by *Butler et al.* [1999] for the first half of the twentieth century based on the South Pole firn air data.

[13] It should be noted that CH_3Br is unstable toward hydrolysis and chloride substitution in aqueous solution [*Moelwyn-Hughes*, 1938; *Elliott and Rowland*, 1995; *King and Saltzman*, 1997] and there is potential for similar chemistry in snow and ice. From these data, we cannot rule out the possibility that CH_3Br slowly degrades in firn and ice. Longer ice core records are needed to fully assess this issue.

3. Model Simulations of Preindustrial CH_3Br

3.1. Model Description

[14] A numerical model was developed in order to provide a basis for comparison of the ice core results with our current understanding of the atmospheric CH_3Br budget. This model simulates the major processes involved in the global biogeochemical cycle of CH_3Br, including oceanic production and consumption, soil uptake, terrestrial plant emissions, fumigation, gasoline combustion, biomass burning, atmospheric loss via reaction with OH and photolysis in the stratosphere. The model is time-dependent and is run for several years to obtain "equilibrium" simulations for modern (1995–1998) and preindustrial conditions, assuming various emissions scenarios. In this model, the atmosphere is represented by well-mixed Northern and Southern Hemisphere tropospheric boxes, and transport between them is governed by an interhemispheric exchange

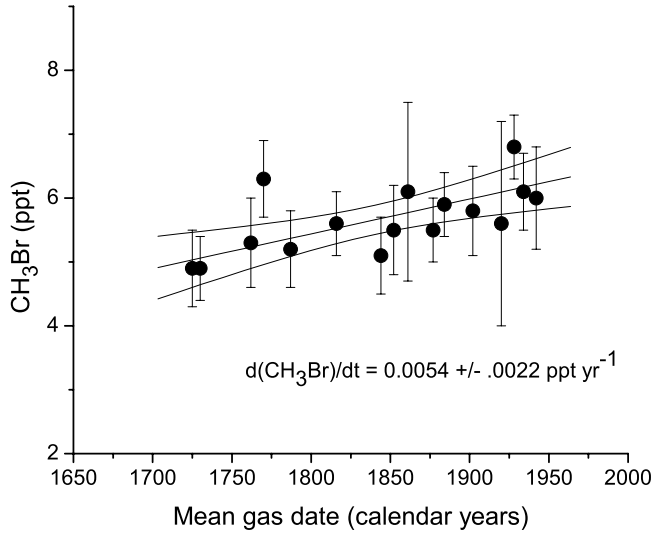

Figure 3. Weighted, least squares, linear regression of ice core CH_3Br measurements against time. The deepest ice core measurement and six outliers were removed from the data set, as discussed in the text.

Table 1. Various Parameters Specified in the Model for Both Modern and Preindustrial Simulations[a]

	Southern Hemisphere	Northern Hemisphere
Atmospheric Loss Rate Constants, yr^{-1}		
OH	0.51	0.60
Soils	0.18	0.44
Stratospheric photolysis	0.03	0.03
Interhemispheric exchange	1.00	1.00
Oceanic Loss Rate Constants, yr^{-1}		
CH_3Br production rate, pM d^{-1}	0.17	0.29
Water column loss rate constant, d^{-1}	0.18	0.25

[a]Atmospheric terms are based on *Montzka et al.* [2003b], and ocean terms are based on *Yvon-Lewis and Butler* [1997], with modifications as described in text.

time constant of one year. Modern source and sink fluxes are consistent with the budget as described by *Montzka et al.* [2003b] after adjusting the sinks and corresponding oceanic emission terms for the 1995–1998 mean tropospheric mixing ratio of 9.37 ppt [*Montzka et al.*, 2003a]. This mixing ratio yields a tropospheric CH_3Br burden of 130 Gg and a total atmospheric CH_3Br burden of 137 Gg [*Montzka et al.*, 2003a]. The three-dimensional global model of *Lee-Taylor et al.* [1998] and the two-dimensional model of *Reeves* [2003] use the 146 Gg CH_3Br atmospheric burden from *Kurylo et al.* [1999] and *Montzka et al.* [2003b] and do not include all of the terrestrial sources included in this model. Hemispheric average rate constants used in the model are listed in Table 1. The 1 year interhemispheric exchange time constant used in the model is well calibrated for midlatitude sources, but it most likely underestimates the rate of interhemispheric transport of emissions from tropical sources, such as biomass burning, plant emissions, and tropical ocean air/sea exchange.

[15] The atmospheric loss of CH_3Br via OH is calculated by integrating the monthly mean OH fields of *Spivakovsky et al.* [2000] with the rate constant from *De More et al.* [1997]. A minor additional loss from stratospheric photolysis was estimated assuming a rate constant of 0.029 yr^{-1} for each tropospheric box [*Kaye et al.*, 1994].

[16] The oceans are treated as a $1^\circ \times 1^\circ$ grid of ocean cells extending from the surface to the base of the mixed layer [*Yvon-Lewis and Butler*, 2002]. Monthly average ocean parameters from the NOAA/GFDL Global Oceanographic Data Set Atlas (available at http://dss.ucar.edu/datasets/ds279.0) were used to characterize oceanic temperatures, salinities, mixed layer depths, and 10 m wind speeds. Thermocline diffusivities were obtained from *Li et al.* [1984]. Air/sea gas exchange coefficients were calculated from the quadratic relationship of *Wanninkhof* [1992]. A mass balance for CH_3Br was computed for each grid cell using the parameterization of *Yvon-Lewis and Butler* [1996]. The rate expression of *King and Saltzman* [1997] was used to calculate chemical loss, and a uniform biological degradation rate constant of 0.05 d^{-1} was assumed [*Tokarczyk and Saltzman*, 2001; *Tokarczyk et al.*, 2001]. The solubility and diffusivity of CH_3Br were obtained from *De Bruyn and Saltzman* [1997a, 1997b]. Monthly values of water column production rates for CH_3Br in each grid cell were specified to obtain agreement with the observed distribution of saturation anomalies in the oceans, as parameterized by *King et al.* [2002], and with the monthly mean tropospheric hemispheric 1995–1998 mixing ratios [*Montzka et al.*, 2003a]. The approach of calculating the steady-state surface ocean production needed to achieve a given sea surface saturation state has been used in several previous global CH_3Br models. *Anbar et al.* [1996] and *Pilinis et al.* [1996] used chlorophyll-based or constant production terms scaled to achieve agreement with the existing data base for sea surface saturation state, which at that time was considerably more limited than today. *Lee-Taylor et al.* [1998] utilized a latitude-based parameterization of sea surface saturation state, which was constant throughout the year. *Reeves* [2003] used the *King et al.* [2000] SST-based parameterization of sea surface saturation state, which provides one relationship for the entire year. The *King et al.* [2002] parameterization used in this study estimates sea surface saturation state using two seasonal SST-based relationships to provide a better fit to midlatitude data.

[17] The uptake of CH_3Br from the atmosphere by soils is based on the laboratory studies by *Shorter et al.* [1995] and *Varner et al.* [1999b]. These authors extrapolated the laboratory data using the global distribution of soil biomes of *Born et al.* [1990] to obtain a global uptake rate of 47 Gg yr^{-1} [*Yvon-Lewis*, 2000; *Montzka et al.*, 2003b]. This global uptake rate was recalculated on the basis of the adjustment in the atmospheric burden discussed above, giving 41.7 Gg yr^{-1}. We apportioned their global soil uptake rate constant between the Northern and Southern Hemispheres using the hemispheric distribution of biome types given by *Matthews* [1983]. Soil uptake is parameterized in the model as a first-order loss rate constant specified for each hemisphere. Seasonality was modeled after *Shorter et al.* [1995] by assigning "active" and "inactive" months to the various biomes.

[18] The biomass-burning source for the modern atmosphere is based on the $\Delta CH_3Br/\Delta CO_2$ emissions ratios estimated by *Mano and Andreae* [1994] and *Andreae et al.* [1996]. The seasonality and hemispheric distributions of biomass-burning emissions are as given by *Granier et al.* [1996] and *Lee-Taylor et al.* [1998]. The total emissions from fumigation of soils, durables, perishables, and structures and from gasoline combustion are 45.8 Gg yr^{-1} [*Kurylo et al.*, 1999]. The hemispheric distribution and seasonality of these sources in the model is based on government and industry statistics, as given by *Lee-Taylor et al.* [1998].

[19] The current best estimate for global plant emissions is about 24 Gg yr^{-1} [*Montzka et al.*, 2003b]. The global rapeseed emissions estimated by *Gan et al.* [1998] are distributed between the two hemispheres in proportion to the distribution of cultivated land cover from *Matthews* [1983]. The global salt marsh emissions from *Rhew et al.* [2000] are distributed between the hemispheres according to the salt marsh distribution in the International Satellite Land Surface Climatology Project (ISLSCP) [*Meeson et al.*, 1995; *Sellers et al.*, 1995]. The global shrubland emissions from *Rhew et al.* [2001] are distributed between the hemispheres according to the shrubland distribution of *Matthews* [1983]. The global wetland emissions from *Varner et al.* [1999a] are distributed between the hemispheres according to the wetland distribution in the ISLSCP. The active season

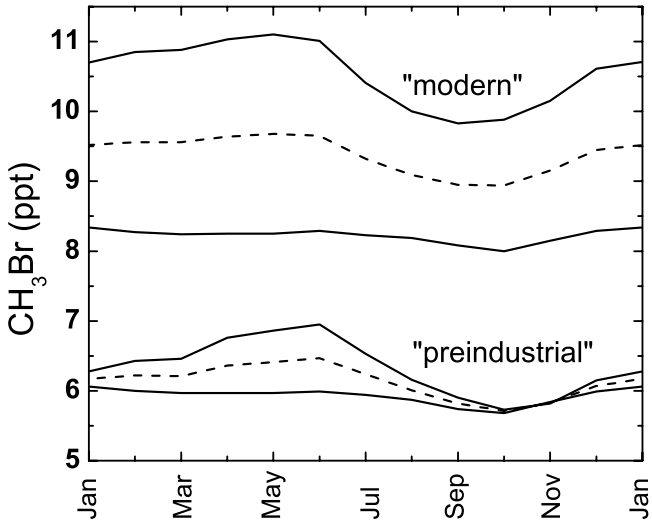

Figure 4. Model simulation of atmospheric CH_3Br using the "modern" and case 2 "preindustrial" scenarios. For each simulation, the upper and lower solid lines are results for the Northern and Southern Hemispheres, respectively. The dashed lines are the global average results for each simulation.

for these terrestrial sources is assumed to be the warmest 240 days in each hemisphere. The global fungus emissions from *Lee-Taylor and Holland* [2000] are distributed between the hemispheres according to the tropical forest distribution of *Matthews* [1983], and the active season for this emission is assumed to be 365 days.

[20] Peatlands and rice paddies [*Redeker et al.*, 2000; *Dimmer et al.*, 2001] are not included as independent sources in this model. These land cover types are classified as wetlands in the ISLSCP land cover databases. When a suitable land cover database is available, reclassifying some of the wetlands as peatlands and rice paddies will result in a small reduction in "known" global emissions.

[21] The model is integrated using an explicit, variable time step, Runge-Kutta algorithm [*Bogacki and Shampine*, 1989]. The model is integrated for several years, until it reaches an annual steady state.

[22] There is a significant imbalance in the "best estimate" CH_3Br budget [*Montzka et al.*, 2003b], with atmospheric losses exceeding the known sources by 37.6 Gg yr^{-1} after adjusting to the 128 Gg atmospheric burden and removing peatland and rice paddy emissions. The magnitude of the unknown source(s) was adjusted in the model to achieve agreement with the mean 1995–1998 tropospheric hemispheric mixing ratios of 10.5 (NH) and 8.2 (SH) ppt and their seasonalities [*Montzka et al.*, 2003a]. This required additional emissions of 18.3 and 19.3 Gg yr^{-1} in the Northern and Southern Hemispheres, respectively. In each hemisphere, the seasonality of this unknown source was adjusted to match the seasonality of the monthly mean mixing ratios. It is likely that at least some of the imbalance between sources and sinks is attributable to emissions from terrestrial plants. To date, only limited emissions surveys from terrestrial plants and ecosystems have been carried out [*Gan et al.*, 1998; *Redeker et al.*, 2000; *Rhew et al.*, 2000, 2001; *Varner et al.*, 1999a; *Dimmer et al.*, 2001; *Yokouchi et al.*, 2002]. The imbalance could also result from underestimating anthropogenic emissions, but this explanation cannot account for the imbalance in the Southern Hemisphere, as demonstrated below using model results.

3.2. Model Results and Discussion

[23] The model described above was used to carry out simulations of atmospheric CH_3Br using a "modern" scenario and four "preindustrial" scenarios. The modern case utilizes the best estimate parameterizations for all sources and sinks including the additional unknown source (Figure 4). The unknown source is adjusted in order to balance the global budget, and to agree with atmospheric observations in both hemispheres in terms of mean levels and seasonality [*Cicerone et al.*, 1988; *Wingenter et al.*, 1998; *Montzka et al.*, 2003a]. Note the marked difference in seasonality between the two hemispheres. The Northern Hemisphere has a seasonal amplitude greater than 1 ppt, with the late summertime minimum and late wintertime maximum expected for a gas whose dominant sink is reaction with OH. The Southern Hemisphere has a much smaller seasonal amplitude. At least in part, this behavior reflects the importance of the oceans in the Southern Hemisphere budget. The Southern Hemisphere oceans vary seasonally from a large net sink during winter to a small net source during summer, offsetting the influence of atmospheric OH. The hemispheric mean annual net fluxes of CH_3Br into and out of the atmosphere are shown in Table 2.

[24] A "preindustrial" scenario (case 1) was constructed starting from the modern budget and setting the fumigation and gasoline combustion sources to zero. The unknown source needed to balance the modern CH_3Br budget is included in this scenario. This scenario yields a preindustrial southern hemispheric CH_3Br level of 6.6 ppt, slightly higher than the ice core measurements. Eliminating the current best estimate of anthropogenic emissions is insufficient to explain the preindustrial ice core levels, assuming that all of the unknown source was present in preindustrial times. This result suggests that either these components of the budget underestimate the anthropogenic input while overpredicting natural sources or that some of the natural sources have changed over the past century.

[25] A second preindustrial scenario (case 2) was constructed by (1) eliminating the anthropogenic sources as in case 1 and (2) decreasing global biomass-burning emissions to 25% of their modern value, from 20 to 5 Gg yr^{-1}. As above, the unknown source is included in this scenario. This simulation yields a preindustrial southern hemispheric CH_3Br level of 5.9 ppt, in close agreement to the ice core measurements. Today, the majority of biomass burning is carried out in the tropics to clear forested land for agricultural use. It seems likely that this burning source would have been significantly lower during preindustrial times. However, to our knowledge, there is no objective basis for estimating preindustrial biomass-burning rates.

[26] A third preindustrial scenario (case 3) was run to illustrate the uncertainty associated with the imbalance in the CH_3Br budget. In this case, fumigation and combustion sources in the CH_3Br budget are set to zero as in case 1. In addition, we assume that all of the unknown emissions in the Northern Hemisphere, 18.3 Gg yr^{-1}, are anthropogenic and remove them from the budget. An additional 1.3 Gg yr^{-1} of

Table 2. Hemispheric Budget Estimates for Atmospheric CH_3Br for Modern and Preindustrial Model Simulations, Based on *Montzka et al.* [2003b][a]

	Modern Scenario, Global Mean 9.4 ppt		Preindustrial Scenarios							
			Global Mean for Case 1: 6.9 ppt		Global Mean for Case 2: 6.1 ppt		Global Mean for Case 3: 5.9 ppt		Global Mean for Case 4: 4.9 ppt	
	SH	NH	SH	NH	SH	NH	SH	NH	SH	NH
Hemispheric mean, ppt	8.2	10.5	6.6	7.3	5.9	6.3	5.9	5.9	4.5	5.3
Sources/sinks, Gg yr^{-1}										
Fumigation, combustion	3.2	42.6	0	0	0	0	0	0	0	0
Biomass burning	5.9	14.1	5.9	14.1	1.5	3.5	5.9	14.1	5.9	14.1
Terrestrial vegetation	4.7	23.8	4.7	23.8	4.7	23.8	4.7	23.8	4.7	23.8
Unidentified sources	19.3	18.3	19.3	18.3	19.3	18.3	18.0	0	0	0
OH and hν	−30.3	−45.4	−24.3	−31.4	−21.8	−27.5	−21.8	−25.5	−16.7	−23.8
Soils	−10.2	−31.8	−8.2	−22.1	−7.3	−19.4	−7.3	−18.0	−5.7	−16.2
Ocean (net)	−8.60	−5.8	−2.0	1.9	0.8	4.1	0.9	5.2	6.5	6.6
Interhemispheric exchange	15.9	−15.9	4.6	−4.6	2.9	−2.9	0.3	−0.3	5.3	−5.3

[a]The preindustrial scenarios are as follows: case 1, no anthropogenic emissions; case 2, no anthropogenic emissions, 75% reduction in biomass-burning emissions; case 3, no anthropogenic emissions, assuming all of the modern unidentified source in the Northern Hemisphere is anthropogenic; case 4, no anthropogenic emissions, assuming all of the modern unidentified source in both hemispheres is anthropogenic. SH, Southern Hemisphere; NH, Northern Hemisphere.

the unidentified emissions in the Southern Hemisphere are also designated as anthropogenic, on the basis of the estimate that 7% of the global anthropogenic emissions are believed to occur in the Southern Hemisphere. This simulation results in a Southern Hemisphere CH_3Br level of 5.9 ppt, which is also consistent with the ice core results. This result demonstrates that the ice core data do not a priori preclude a significantly larger anthropogenic contribution to the modern CH_3Br budget than assumed in the best estimate budget of *Montzka et al.* [2003b]. However, this scenario requires that biomass-burning emissions remain constant, and that the remaining 18.0 Gg yr^{-1} flux of unidentified sources occurs only within the Southern Hemisphere.

[27] A fourth preindustrial scenario (case 4) was run to illustrate the sensitivity of southern hemispheric atmospheric CH_3Br mixing ratios to the unknown source in that hemisphere. In this case the emissions are the same as in case 3, but we also remove the remaining 18.0 Gg yr^{-1} unknown source from the budget. This scenario gives a Southern Hemisphere CH_3Br level of 4.5 ppt, which is below the ice core results. This result demonstrates that there must have been an unidentified southern hemispheric source of CH_3Br to the preindustrial atmosphere. This result is consistent with the model results of *Reeves* [2003] based on the firn air data.

[28] In these simulations, the atmospheric burden of CH_3Br does not respond linearly to a change in anthropogenic emissions. For example, in the case 2 and case 3 preindustrial budgets, the total net emissions into the atmosphere are about 71 and 67 Gg yr^{-1}. The modern budget contains an additional 61–64 Gg yr^{-1}. Therefore one might expect the atmospheric CH_3Br burden to have nearly doubled (increase by a factor of 1.9) between preindustrial and modern times. The model response to addition of the anthropogenic sources was an increase of only 3.5 ppt, or a factor of about 1.6. The ''missing'' anthropogenic CH_3Br, about 20 Gg, was taken up by the oceans. For the preindustrial scenarios, the oceans ranged from a small net sink (case 1) to a large net source (cases 2–4). The increasing atmospheric burden caused by anthropogenic emissions caused the oceans to become a large net sink for atmospheric CH_3Br. This coupling between the oceans and atmosphere has the effect of stabilizing the atmosphere against increases caused by terrestrial or anthropogenic emissions, as described by *Butler* [1994].

[29] In these scenarios we have not addressed the possibility of preindustrial/industrial changes in atmospheric CH_3Br lifetime resulting from changes in atmospheric OH. Although there is little consensus as to the magnitude (or even the sign) of such changes, model calculations suggest that tropospheric OH has changed by less than 20% during the industrial era. *Wang and Jacob* [1998] argued that the effect of such changes on the atmospheric lifetimes of most gases is negligible. In their model, decreasing global mean OH during the past century was offset by increasing OH levels in the warmer lower troposphere, where most oxidation of CH_3Br occurs. This effect is further reduced because OH is only responsible for roughly half of the total atmospheric loss of CH_3Br, i.e., a change of 10% in the partial lifetime of CH_3Br with respect to OH, would cause a change of about 6% in the total lifetime of CH_3Br or in its atmospheric levels.

4. Implications

[30] Together, the ice core and firn air measurements and the model simulations provide a reasonably consistent picture of how anthropogenic activities have modified the atmospheric CH_3Br burden during the past century. Over that time, the global atmospheric burden appears to have increased by 3.5 ppt, or roughly 50% of the preindustrial level. The major uncertainty in the modern atmospheric budget of CH_3Br remains the fact that the known sinks exceed the known sources. It is important to determine whether the unidentified CH_3Br sources are anthropogenic or natural. We can state conclusively that not all of the unidentified emissions can be treated as anthropogenic. If all of the 37.6 Gg yr^{-1} of unknown emissions in the modern budget were treated as anthropogenic, the preindustrial scenario would give a Southern Hemisphere atmospheric level of about 4.5 ppt (Table 2), well below the ice core measurements.

[31] The model simulations show that the ice core data alone is insufficient to determine whether the unidentified

source was present in the preindustrial northern hemispheric budget or not. The model does clearly show that a large unidentified source is needed in the preindustrial Southern Hemisphere. The limitations on our ability to constrain the preindustrial atmospheric CH_3Br budget stem largely from the fact that ice core data are available for the Southern Hemisphere only, and the lack of an objective basis on which to assign preindustrial biomass-burning emissions.

[32] The analysis presented here implicitly assumes that the natural components of the budget remained constant. This assumption may not necessarily be justified. It is also possible that human activities, particularly land use practices, may alter emissions from terrestrial vegetation in ways that are not accounted for in the budget. It seems likely that variations in climatic conditions would have a marked impact on plant emissions, soil uptake, and oceanic production. Longer ice core records including periods of major climate change may reveal the impact of climate variability on the CH_3Br budget.

[33] **Acknowledgments.** We wish to thank Jim Butler, Steve Montzka, Rob Rhew, Ryszard Tokarczyk, Mark Battle, Michael Bender, and Michael Prather for helpful discussions. We also wish to thank Ken Taylor, Mark Twickler, and the staff of the WAISCORES project and NICL. This research was supported by the Office of Polar Programs and the Chemical Oceanography Programs at the National Science Foundation.

References

Anbar, A. D., Y. L. Yung, and F. P. Chavez (1996), Methyl bromide: Ocean sources, ocean sinks, and climate sensitivity, *Global Biogeochem. Cycles*, *10*, 175–190.

Andreae, M. O., et al. (1996), Methyl halide emissions from savanna fires in southern Africa, *J. Geophys. Res.*, *101*, 23,603–23,613.

Aydin, M., W. J. De Bruyn, and E. S. Saltzman (2002), Preindustrial atmospheric carbonyl sulfide (OCS) from an Antarctic ice core, *Geophys. Res. Lett.*, *29*(9), 1359, doi:10.1029/2002GL014796.

Aydin, M., E. S. Saltzman, W. J. De Bruyn, S. A. Montzka, J. H. Butler, and M. Battle (2004), Atmospheric variability of methyl chloride during the last 300 years from an Antarctic ice core and firn air, *Geophys. Res. Lett.*, *31*, L02109, doi:10.1029/2003GL018750.

Bogacki, P., and L. F. Shampine (1989), A 3(2) pair of Runge-Kutta formulas, *Appl. Math. Lett.*, *2*, 1–9.

Born, M., H. Dörr, and I. Levin (1990), Methane consumption in aerated soils of the temperate zone, *Tellus, Ser. B*, *42*, 2–8.

Butler, J. H. (1994), The potential role of the ocean in regulating atmospheric CH_3Br, *Geophys. Res. Lett.*, *21*, 185–188.

Butler, J. H., et al. (1999), A record of atmospheric halocarbons during the twentieth century from polar firn air, *Nature*, *399*, 749–755.

Cicerone, R. J., L. E. Heidt, and W. H. Pollock (1988), Measurements of atmospheric methyl bromide and bromoform, *J. Geophys. Res.*, *93*, 3745–3749.

De Bruyn, W. J., and E. S. Saltzman (1997a), The solubility of methyl bromide in pure water, 35 ppt sodium chloride and seawater, *Mar. Chem.*, *56*, 51–57.

De Bruyn, W. J., and E. S. Saltzman (1997b), Diffusivity of methyl bromide in water, *Mar. Chem.*, *57*, 55–59.

De More, W. B., S. P. Sander, D. M. Golden, R. F. Hampson, M. J. Kurylo, C. J. Howard, A. R. Ravishankara, C. E. Kolb, and M. J. Molina (1997), Chemical kinetics and photochemical data for use in stratospheric modeling: Evaluation number 12, *JPL Publ., 97-4*.

Dimmer, C. H., P. G. Simmonds, G. Nickless, and M. R. Bassford (2001), Biogenic fluxes of halomethanes from Irish peatland ecosystems, *Atmos. Environ.*, *35*, 321–330.

Elliott, S., and F. S. Rowland (1995), Methyl halide hydrolysis rates in natural waters, *J. Atmos. Chem.*, *20*, 229–236.

Etheridge, D. M., et al. (1996), Natural and anthropogenic changes in atmospheric CO_2 over the last 1000 years from air in Antarctic ice and firn, *J. Geophys. Res.*, *101*, 4115–4128.

Gan, J., S. R. Yates, H. D. Ohr, and J. J. Sims (1998), Production of methyl bromide by terrestrial higher plants, *Geophys. Res. Lett.*, *25*, 3595–3598.

Granier, C., W.-M. Hao, G. Brasseur, J.-F. and Muller (1996), Land use practices and biomass burning: Impact on the chemical composition of the atmosphere, in *Biomass Burning and Global Change*, edited by J. S. Levine, pp. 140–148, MIT Press, Cambridge, Mass.

Kaye, J. A., S. A. Penkett, and F. M. Ormond (Eds.) (1994), Report on concentrations, lifetimes, and trends of CFCs, halons, and related species, *NASA Ref. Publ., 1339*.

Khalil, M. A. K., R. A. Rasmussen, and R. Gunawardena (1993), Atmospheric methyl bromide: Trends and global mass balance, *J. Geophys. Res.*, *98*, 2887–2896.

King, D. B., and E. S. Saltzman (1997), Removal of methyl bromide in coastal seawater: Chemical and biological rates, *J. Geophys. Res.*, *102*, 18,715–18,721.

King, D. B., J. H. Butler, S. A. Montzka, S. A. Yvon-Lewis, and J. W. Elkins (2000), Implications of methyl bromide supersaturations in the temperate North Atlantic Ocean, *J. Geophys. Res.*, *105*, 19,763–19,769.

King, D. B., J. H. Butler, S. A. Yvon-Lewis, and S. A. Cotton (2002), Predicting oceanic methyl bromide saturation from SST, *Geophys. Res. Lett.*, *29*(24), 2199, doi:10.1029/2002GL016091.

Kurylo, M. J., et al. (1999), Short-lived ozone-related compounds, in *Scientific Assessment of Ozone Depletion: 1998*, *Global Ozone Res. Monit. Proj. Rep. 44*, chap. 2, pp. 2.1–2.56, World Meteorol. Organ., Geneva.

Lee-Taylor, J. M., and E. A. Holland (2000), Litter decomposition as a potential natural source of methyl bromide, *J. Geophys. Res.*, *105*, 8857–8864.

Lee-Taylor, J. M., S. C. Doney, G. P. Brasseur, and J.-F. Muller (1998), A global three-dimensional atmosphere-ocean model of methyl bromide distributions, *J. Geophys. Res.*, *103*, 16,039–16,057.

Li, Y. H., T. H. Peng, and W. S. Broecker (1984), The average vertical mixing coefficient for the oceanic thermocline, *Tellus, Ser. B*, *36*, 212–217.

Mano, S., and M. O. Andreae (1994), Emission of methyl bromide from biomass burning, *Science*, *263*, 1255–1257.

Matthews, E. (1983), Global vegetation and land use: New high-resolution databases for climate studies, *J. Clim. Appl. Meteorol.*, *22*, 474–487.

Meeson, P. J., F. E. Corprew, J. M. P. McManus, D. M. Mayers, J. W. Closs, K.-J. Sun, D. J. Sunday, and P. J. Sellers (1995), ISLSCP Initiative I-Global data sets for land-atmosphere models, 1987–1988 (CD-ROM), vol. 1–5, *USA_NASA_GDAAC_ISLSCP_001-USA_NASA_GDAAC_ISLSCP_005*, http://daac.gsfc.nasa.gov/, Distrib. Active Arch. Cent., Greenbelt, Md.

Miller, B. R. (1998), Abundances and trends of atmospheric chlorodifluoromethane and bromomethane, Ph.D. thesis, Univ. of Calif., San Diego.

Moelwyn-Hughes, E. A. (1938), The hydrolysis of the methyl halides, *Proc. R. Soc. London, Ser. A*, *164*, 295–306.

Montzka, S. A., J. H. Butler, B. D. Hall, D. J. Mondeel, and J. W. Elkins (2003a), A decline in tropospheric organic bromine, *Geophys. Res. Lett.*, *30*(15), 1826, doi:10.1029/2003GL017745.

Montzka, S. A., et al. (2003b), Controlled substances and other source gases, in *Scientific Assessment of Ozone Depletion: 2002*, chap. 1, pp. 1.1–1.83, *Global Ozone Res. Monit. Proj. Rep. 47*, World Meteorol. Organ., Geneva.

Pilinis, C., D. B. King, and E. S. Saltzman (1996), The oceans: A source or a sink of methyl bromide?, *Geophys. Res. Lett.*, *23*, 817–820.

Redeker, K. R., N. Y. Wang, J. C. Low, A. McMillan, S. C. Tyler, and R. J. Cicerone (2000), Emissions of methyl halides and methane from rice paddies, *Science*, *290*, 966–969.

Reeves, C. E. (2003), Atmospheric budget implications of the temporal and spatial trends in methyl bromide concentration, *J. Geophys. Res.*, *108*(D11), 4343, doi:10.1029/2002JD002943.

Rhew, R. C., B. R. Miller, and R. F. Weiss (2000), Natural methyl bromide and methyl chloride emissions from coastal salt marshes, *Nature*, *403*, 292–295.

Rhew, R. C., B. R. Miller, M. K. Vollmer, and R. F. Weiss (2001), Shrubland fluxes of methyl bromide and methyl chloride, *J. Geophys. Res.*, *106*, 20,875–20,882.

Schwander, J. (1989), The transformation of snow to ice and the occlusion of gases, in *The Environmental Record in Glaciers and Ice Sheets*, pp. 53–67, Wiley-Interscience, New York.

Schwander, J., B. Stauffer, and A. Sigg (1988), Air mixing in firn and the age of the air at pore close-off, *Ann. Glaciol.*, *10*, 141–145.

Sellers, P. J., et al. (1995), An overview of the ISLSCP Initiative I global data sets for land-atmosphere models, 1987–1988, vol. 1–5, vol. 1: *USA_NASA_GDAAC_ISLSCP_001, OVERVIEW.DOC*, http://daac.gsfc.nasa.gov/, Distrib. Active Arch. Cent., Greenbelt, Md.

Shorter, J. H., C. E. Kolb, P. M. Crill, R. A. Kerwin, R. W. Talbot, M. E. Hines, and R. C. Harriss (1995), Rapid degradation of atmospheric methyl bromide in soils, *Nature*, *377*, 717–719.

Spivakovsky, C. M., et al. (2000), Three-dimensional climatological distribution of tropospheric OH: Update and evaluation, *J. Geophys. Res.*, *105*, 8931–8980.

Sturges, W. T., H. P. McIntyre, S. A. Penkett, J. A. Chappellaz, J.-M. Barnola, R. Mulvaney, E. Atlas, and V. Stroud (2001), Methyl bromide, other brominated methanes and methyl iodide in polar firn air, *J. Geophys. Res.*, *106*, 1595–1606.

Swanson, A. L., N. J. Blake, J. E. Dibb, M. A. Albert, D. R. Blake, and F. S. Rowland (2002), Photochemically induced production of CH_3Br, CH_3I, C_2H_5I, ethene, and propene within surface snow, *Atmos. Environ.*, *36*, 2671–2682.

Tans, P. P., et al. (2001), Carbon cycle, in *Climate Monitoring and Diagnostics Laboratory Summary Report 25*, *1998–1999*, edited by R. Schnell, D. King, and R. Rosson, chap. 2, pp. 25–46, Natl. Oceanic and Atmos. Admin., Boulder, Colo.

Tokarczyk, R., and E. S. Saltzman (2001), Methyl bromide loss rates in surface waters of the North Atlantic Ocean, Caribbean Sea, and eastern Pacific Ocean (8–45°N), *J. Geophys. Res.*, *106*, 9843–9851.

Tokarczyk, R. K., D. Goodwin, and E. S. Saltzman (2001), Methyl bromide loss rate constants in the North Pacific Ocean (11–57°N), *Geophys. Res. Lett.*, *28*, 4429–4432.

Trudinger, C. M., et al. (1997), Modelling air movement and bubble trapping in firn, *J. Geophys. Res.*, *102*, 6747–6763.

Varner, R. K., P. M. Crill, and R. W. Talbot (1999a), Wetlands: A potentially significant source of atmospheric methyl bromide and methyl chloride, *Geophys. Res. Lett.*, *26*, 2433–2436.

Varner, R. K., P. M. Crill, R. W. Talbot, and J. H. Shorter (1999b), An estimate of uptake of atmospheric methyl bromide by agricultural soils, *Geophys. Res. Lett.*, *26*, 727–730.

Walker, S. J., R. F. Weiss, and P. K. Salameh (2000), Reconstructed histories of the annual mean atmospheric mole fractions for the halocarbons CFC-11, CFC-12, CFC-113, and carbon tetrachloride, *J. Geophys. Res.*, *105*, 14,285–14,296.

Wang, Y., and D. J. Jacob (1998), Anthropogenic forcing on tropospheric ozone and OH since preindustrial times, *J. Geophys. Res.*, *103*, 31,123–31,135.

Wanninkhof, R. (1992), Relationship between wind speed and gas exchange over the ocean, *J. Geophys. Res.*, *97*, 7373–7382.

Wilke, C. R., and C. Y. Lee (1955), Estimation of diffusion coefficients for gases and vapours, *Ind. Eng. Chem.*, *47*, 1253–1257.

Wingenter, O. W., C. J. L. Wang, D. R. Blake, and F. S. Rowland (1998), Seasonal variations of tropospheric methyl bromide concentrations: Constraints on anthropogenic input, *Geophys. Res. Lett.*, *25*, 2797–2800.

Yokouchi, Y., D. Toom-Sauntry, K. Yazawa, T. Inagaki, and T. Tamaru (2002), Recent decline of methyl bromide in the troposphere, *Atmos. Environ.*, *36*, 4985–4989.

Yvon-Lewis, S. A. (2000), Methyl bromide in the atmosphere and ocean, *IGACtivities Newslett.*, *19*, 9–12.

Yvon-Lewis, S. A., and J. H. Butler (1996), An improved estimate of the oceanic lifetime of atmospheric CH_3Br, *Geophys. Res. Lett.*, *23*, 53–56.

Yvon-Lewis, S. A., and J. H. Butler (1997), The potential effect of oceanic biological degradation on the lifetime of atmospheric CH_3Br, *Geophys. Res. Lett.*, *24*, 1227–1230.

Yvon-Lewis, S. A., and J. H. Butler (2002), Effect of oceanic uptake on atmospheric lifetimes of selected trace gases, *J. Geophys. Res.*, *107*(D20), 4414, doi:10.1029/2001JD001267.

M. Aydin and E. S. Saltzman, Earth System Science, University of California, Irvine, 220 Rowland Hall, Irvine, CA 92697-3100, USA. (maydin@uci.edu; esaltzma@uci.edu)

W. J. De Bruyn, Department of Physical Sciences, Chapman University, Orange, CA 92866, USA. (dbruyn@chapman.edu)

D. B. King, Department of Chemistry, Drexel University, 3141 Chestnut Street, Philadelphia, PA 19104, USA. (daniel.king@drexel.edu)

S. A. Yvon-Lewis, Atlantic Oceanographic and Meteorological Laboratory, NOAA, 4301 Rickenbacker Causeway, Miami, FL 33149-1026, USA. (shari.yvon-lewis@noaa.gov)